Wavelet analysis of the energy transfer caused by convective terms: Application to the Burgers shock

Makoto Iima and Sadayoshi Toh
Division of Physics and Astronomy, Graduate School of Science, Kyoto University, Kyoto 606-01, Japan
(Received 16 January 1995; revised manuscript received 2 August 1995)

Orthonormal wavelet analysis, which can deal with the information about both space and scale simultaneously, is applied to analyze the energy transfer due to spatial structures. To utilize the concept of "triad interaction" in non-Fourier bases, a simple and appropriate definition of transfer functions is proposed. An essential problem in the use of orthogonal wavelets is a fast oscillation observed in the temporal variations of energy and transfer functions. This oscillation is intrinsic to a wavelet base function and corresponds to "phase" in spatial information. A way to remove the phase is also proposed. These prescriptions are applied to examine the energy transfer process of the Burgers shock as a preliminary work. It is shown that the energy transfer is well separated into ones caused by the mean flow and the velocity field of the shock. Within a scale, those correspond to sweeping and compression, respectively. The mean flow contributes even to the energy transfer across a scale, but it is not substantial.

PACS number(s): 03.40.Gc, 47.27.Ak

I. INTRODUCTION

Spatially intermittent structures play an important role especially when cascade processes are examined dynamically. In the energy cascade process, stretching of vortices causes energy to be transferred toward smaller scales. However, the relation between the dynamics of vortices and the mechanism of cascade has not been clearly understood so far. We would therefore like to confirm what role spatially localized structures play in cascade or general transfer processes. For this purpose we utilize orthonormal wavelet analysis in this paper [1,2]. The wavelet contains information about both scale and position. Therefore it is very convenient for studying the spatial distribution of self-similar sets in a general sense. In fact, many authors applied wavelet analysis to the energy dissipation, singularity, etc. [2–4].

Among them, Meneveau [3] studied directly the energy transfer across scales in detail. He defined energy transfer and flux functions in wavelet space which are analogous to those in Fourier space. One of his main results is that the variation of the local flux is much larger than the mean value. This observation does not mean necessarily that the inverse transfer of energy is common locally, partially because the sweeping of energy does contribute to the flux function. As Meneveau pointed out, the sweeping does not transfer energy between different scales, because the sweeping of a mass of energy in a scale only induces a pair of positive and negative transfers in the direction of its progression. In Fourier analysis, the sweeping effect cannot be explicitly expressed except if the approach of Waleffe is followed, where he asymptotically showed that a pair of extremely nonlocal triads corresponds to the sweeping by the large-scale local flow [5]. Thus we should carefully apply wavelet analysis to the analysis of energy transfer. Moreover orthonormal wavelet analysis involves its own problems to be solved, some of which were pointed out by Meneveau.

Studies on energy cascade so far are mainly based on the triad interaction in Fourier space [5–9]. Application of these Fourier analyses to wavelet analysis is not straightforward. In Fourier space, because of homogeneity, triad interactions are defined naturally. That is, a special set of wave numbers is selected: $\boldsymbol{k}+\boldsymbol{p}+\boldsymbol{q}=\boldsymbol{0}$. Furthermore, after symmetrization of transfer functions the total energy exchanged among modes in this triad is conserved. In this sense, triad interactions can be regarded as an element constituting energy transfer caused by nonlinear interaction. On the other hand, even for orthonormal wavelets, any three wavelet bases can construct a triad, because the product of any two wavelet bases is not a single wavelet base but a combination of wavelet bases. In addition, the energy exchanged in a triad is not conserved [3]. In fact, Eyink tried to study the locality of the energy transfer by means of a continuous wavelet, but failed to remove the large-scale convection effects due to the lack of a detailed energy balance in his representation [10]. Hence we should introduce an alternative definition of transfer functions in the energy equation to utilize a triad as an element for wavelet analysis. The transfer functions defined in this paper will be confirmed to be the simplest extension of those in Fourier analysis.

Analyzing the transfer process due to moving structures with a wavelet brings about another technical problem on oscillation intrinsic to a wavelet base function. Roughly speaking, each wavelet mode possesses also the information about phase as Fourier modes. However, the simple definition of energy, half the squared wavelet coefficient, cannot remove the information about phase perfectly. This problem is essentially the same as that on the spatial oscillation for continuous wavelet transformation with a real-valued wavelet. However, the latter is

well known and the use of a complex-valued wavelet is advised to evade the phase oscillation [4]. On the other hand, we do not know so far of any complex-valued orthonormal wavelet that possesses proper characteristics such as the compactness both in physical and Fourier spaces. Since the orthonormal wavelet is indispensable for triad-interaction analysis of transfer process, we require some way to remove the phase.

For an orthonormal wavelet, it is hard to recognize the spatial oscillation because of the discreteness of the spatial parameters. Therefore such an oscillation has been neither removed nor even considered. Here we intend to reveal the phase oscillation and show how to remove it. To do this, we adopted a single Burgers shock as one of the simplest models. A shock can be understood as discontinuity of velocity and is also a basic element that constitutes one-dimensional turbulence; the energy of a shock is believed to be transferred to smaller scales. The speed of a shock can be controlled by adding local flow: Galilean transformation. By this transformation, spatial information can be changed to temporal. As a result, the energy of a wavelet mode observed at a spatial point shows fast (phase) oscillation blurring the substantial variation according to the motion of a shock (structure) as shown later in the paper. Therefore discussing the transfer with original data obtained by means of a wavelet may lead to erroneous conclusions.

One of the ways to remove the phase oscillation is time averaging over the period of fast oscillation, which is discussed in Sec. IV B 1. Note that for interacting or moving shocks, their velocities are not the same. Thus the time averaging method does not work well. The possibility of a space averaging method, which is suitable for plural shocks (structures), is also discussed in Sec. IV B 2.

Another word of caution should be mentioned regarding the energy transfer due to pressure. In the case of incompressible fluid, pressure can be determined only by the velocity field through a relation such as $\Delta p = -\nabla \cdot (\boldsymbol{u} \cdot \nabla \boldsymbol{u})$. In Fourier analysis, pressure does not work explicitly in the energy transfer. That is, the incompressibility holds even for the velocity of each wavenumber vector, and then the transfer term due to pressure disappears in the energy equation $\widetilde{\boldsymbol{u}^*}(\boldsymbol{k}) \cdot i\boldsymbol{k}\tilde{p}(\boldsymbol{k}) = 0$. In wavelet analysis, these are no longer true, because a wavelet base is not an eigenfunction of differential operator. Physically speaking, in incompressible fluids information is transmitted to infinitely distant points instantaneously and spatially separate points interact through pressure. Here we should solve pressure explicitly and evaluate its effect on the transfer as done by Meneveau [3]. In this paper, however, we focus our attention on the nonlinear terms because transfer of some quantities such as energy in the Burgers equation, entropy in the Boussinesq equations [11,12], and enstrophy in the two-dimensional (2D) Navier-Stokes equations are not dependent on pressure explicitly. The examination of the role of pressure on the transfer process will be left to future works.

The next section is devoted to the review of the orthonormal wavelet. In Sec. III, we propose a definition of transfer functions which satisfies the detailed balance of energy exchanged in a triad. We also show the generalization of triad interactions. These are applied to analysis of shock dynamics in the Burgers equation in Sec. IV. Some analytical results are also given there. In the final section, summary and conclusions are presented.

II. ORTHONORMAL WAVELET

The orthonormal wavelet has two discretized parameters j and m corresponding to position and scale. Taking the discrete dilation in octaves we define the wavelet base function as follows:

$$\psi_j^m(x) = 2^{m/2}\psi_0(2^m x - j) \quad (m, j \in \mathbb{Z}), \tag{2.1}$$

where ψ_0 is a special function called an analyzing wavelet and $\{\psi_j^m | m, j \in \mathbb{Z}\}$ is a complete orthonormal system. Then a function $f(x)$ is expanded with this orthonormal basis in the following form:

$$f(x) = \sum_{m,j} \hat{f}_j^m \psi_j^m(x), \tag{2.2}$$

where $\hat{f}_j^m$ (m, j are integers) is an expansion coefficient (a wavelet coefficient). It should be noted that m is the scale parameter while j indicates the position in the form $j/2^m$. Their orthonormality condition is

$$\int \psi_j^{m*}(x)\psi_{j'}^{m'}(x)dx = \delta_{jj'}\delta_{mm'} \quad (m, j, m', j' \in \mathbb{Z}), \tag{2.3}$$

where δ_{ij} is Kronecker's symbol.

Following Meyer's procedure [1], the analyzing wavelet is defined as follows. First we choose an infinitely differentiable, real function $\tilde{\phi}_0(k)$ which satisfies the following conditions:

$$\tilde{\phi}_0(k) \geq 0, \quad \tilde{\phi}_0(k) = \tilde{\phi}_0(-k), \tag{2.4}$$

$$\tilde{\phi}_0(k) \text{ is monotonically decreasing for } k \geq 0, \tag{2.5}$$

$$\tilde{\phi}_0(k) = 1 \quad (|k| \leq \tfrac{2}{3}\pi),$$

$$\tilde{\phi}_0(k) = 0 \quad (|k| \geq \tfrac{4}{3}\pi),$$

$$\{\tilde{\phi}_0(k)\}^2 + \{\tilde{\phi}_0(k - 2\pi)\}^2 = 1 (\tfrac{2}{3}\pi \leq k \leq \tfrac{4}{3}\pi). \tag{2.6}$$

Then the Fourier transform of the analyzing function $\tilde{\psi}_0(k)$ is defined as

$$\tilde{\psi}_0(k) = \exp\left(-\frac{k}{2}i\right)\sqrt{\left\{\tilde{\phi}_0\left(\frac{k}{2}\right)\right\}^2 - \{\tilde{\phi}_0(k)\}^2}. \tag{2.7}$$

Finally the analyzing wavelet is obtained by its inverse Fourier transform:

$$\psi_0(x) = \frac{1}{2\pi}\int \tilde{\psi}_0(k)e^{ikx}dk. \tag{2.8}$$

The analyzing wavelet is not chosen uniquely so far. In this paper, we employ one constructed by Yamada and Ohkitani [2]. In their construction, $\tilde{\phi}_0$ is defined as

$$\tilde{\phi}_0(k) = [g(k)g(-k)]^{1/2}, \tag{2.9}$$

where

$$g(k) = h\left(\frac{4}{3}\pi - k\right) \Big/ \left[h\left(k - \frac{2}{3}\pi\right) + h\left(\frac{4}{3}\pi - k\right)\right], \tag{2.10}$$

$$h(k) = \exp(-1/k^2)\ (k > 0), \quad h(k) = 0\ (k \le 0). \tag{2.11}$$

The analyzing wavelet is shown in Fig. 1. The absolute value of $\tilde{\psi}_0(k)$ is also shown in Fig. 2.

Not only the analyzing wavelet but every wavelet base is localized in physical space in the sense that it and its derivatives of any order become rapidly decreasing functions (i.e., functions which converge to zero faster than any power function as $|x| \to \infty$). The Fourier transform of a wavelet base has a compact support in Fourier space [2]. When a field is periodic with its period 1 and the spectrum of the field is compact in the region $|k| \le \frac{8}{3}\pi 2^N$, the set of wavelet bases that is necessary to reconstruct the field in physical space is $\{\psi_j^m | 0 \le m \le N, 0 \le j \le 2^N - 1\}$.

From the definition (2.1), the product of the width of a wavelet base in physical space, Δx_m, and its width in Fourier space, Δk_m, is constant for any scale m:

$$\Delta x_m \Delta k_m = C \quad (C \text{ is a constant}). \tag{2.12}$$

Thus, in physical space, Δk_m defines the inverse of the width of the wavelet base. It should be noted that C is a constant but depends on the definitions of Δx_m and Δk_m. In this paper, we set $\Delta x_m = 2^{-m}$, which is the interval between adjacent wavelet bases of scale m.

As seen in Fig. 1, the symmetric point where the analyzing wavelet takes the maximum value is shifted to the right by $\frac{1}{2}$ from the origin. When we observe an event of some moving velocity, say u_0, the time series of its wavelet coefficient for a wavelet base with (m, j) delays by $\Delta x_m/(2u_0)$ from the observation in physical space at $x = 2^{-m}j$. Therefore we define the representative position of a wavelet base with (m, j) as $x_{m,j} = 2^{-m}(j + \frac{1}{2})$ instead of the usual $2^{-m}j$. It should be noted that the value of the shift, $\Delta x_m/2$, is dependent on the concrete form of the analyzing wavelet. The newly introduced coordinate will be used for the analysis of a shock in Sec. IV and we will see the consistency between our definition and observations.

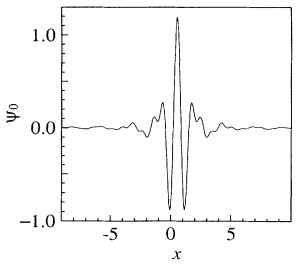

FIG. 1. Meyer's analyzing wavelet.

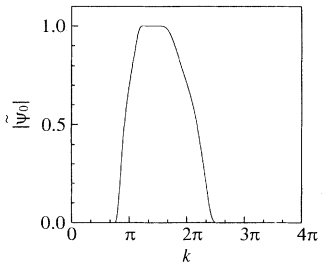

FIG. 2. The absolute values of Fourier coefficients of the analyzing wavelet. The spectrum has a compact support in the region $\frac{2}{3}\pi \le |k| \le \frac{8}{3}\pi$.

III. MATHEMATICAL FORMULATION

A. Definition of transfer function

In this section, we discuss nonlinear interactions and their role in energy transfer based on the Navier-Stokes (NS) equations:

$$\frac{\partial}{\partial t}\boldsymbol{u} = -(\boldsymbol{u}\cdot\nabla)\boldsymbol{u} - \nabla p + \nu\Delta\boldsymbol{u}, \tag{3.1}$$

where p is pressure and ν is the kinetic viscosity. Here we assume that fluid is contained in the periodic box so that velocity is periodic on the boundaries. Generally the box can be extended infinitely where velocity vanishes at infinity.

The strong nonlinear terms in NS equations cause enstrophy or energy transfer from larger to smaller scales in two or three dimensions. In the energy equations, these terms turn into the third order nonlinear terms with respect to velocity, which are called transfer functions. Assume velocity is decomposed into several orthogonal subspaces, e.g., a space spanned by a set of orthonormal wavelet bases:

$$\boldsymbol{u} = \boldsymbol{u}^{(a)} + \boldsymbol{u}^{(b)} + \cdots, \tag{3.2}$$

where we call each part of the right-hand-side a mode, and modes satisfy the orthogonal relation $\int dV \boldsymbol{u}^{(a)} \cdot \boldsymbol{u}^{(b)} = 0$ when $a \ne b$. Then the transfer functions are the combination of all the products of any three

modes. Here we define the energy of the mode as $E^{(a)} \equiv \int |\boldsymbol{u}^{(a)}|^2/2dV$. Time evolution of the energy of the mode c is

$$\frac{d}{dt}E^{(\mathbf{c})} = \sum_{a,b} \mathcal{T}(a : b \to c) + \cdots, \tag{3.3}$$

where the first term on the right-hand side represents the transfer functions due to the nonlinear term (the advection term in this case) in Eq. (3.1). In the case that the surface integrals vanish, we can define the function $\mathcal{T}(a : b \to c)$ as

$$\mathcal{T}(a : b \to c) \equiv -\frac{1}{2}\int dV\{\boldsymbol{u}^{(c)} \cdot (\boldsymbol{u}^{(a)} \cdot \nabla)\boldsymbol{u}^{(b)} - \boldsymbol{u}^{(b)} \cdot (\boldsymbol{u}^{(a)} \cdot \nabla)\boldsymbol{u}^{(c)}\}. \tag{3.4}$$

For convenience' sake, we call this function a unit. In this paper, we regard this unit as a unit expression for energy transfer. We will call mode a a mediating mode, mode b a giving mode, and mode c a receiving mode.

The unit is antisymmetric with respect to the exchange between the modes b and c. Thus the unit can be interpreted as the energy transfer from the mode b to c by a.

By means of the unit we can construct a triad satisfying the detailed energy balance, that is, the energy exchanged among these modes is conserved:

$$T(a|b,c) + T(b|c,a) + T(c|a,b) = 0, \tag{3.5}$$

where

$$T(a|b,c) \equiv \frac{1}{2}\{\mathcal{T}(b : c \to a) + \mathcal{T}(c : b \to a)\},$$
$$T(b|c,a) \equiv \frac{1}{2}\{\mathcal{T}(c : a \to b) + \mathcal{T}(a : c \to b)\},$$
$$T(c|a,b) \equiv \frac{1}{2}\{\mathcal{T}(a : b \to c) + \mathcal{T}(b : a \to c)\}.$$

The function $T(a|b,c)$ is called a detailed transfer function in the Fourier-triad analysis [17]; in Kraichnan's notation $T(a|b,c) = T(a,b,c)$ (see [13]). If the velocity field is decomposed into incompressible subspaces, the unit becomes simpler: $\mathcal{T}(a : b \to c) = -\int dV\{\boldsymbol{u}^{(c)} \cdot (\boldsymbol{u}^{(a)} \cdot \nabla)\boldsymbol{u}^{(b)}\}$. If the Fourier basis is adopted in the definition, the function $T(a|b,c)$ corresponds to the traditional detailed transfer function. Note that nonlinear transfer due to pressure vanishes in this case [14–16].

Furthermore, we define another function by summing units over the mediating mode a:

$$\overline{\mathcal{T}}(b \to c) \equiv \sum_a \mathcal{T}(a : b \to c). \tag{3.6}$$

We call this function the local transfer function. Of course $\overline{\mathcal{T}}(b \to c)$ is antisymmetric between modes b and c.

The unit is not defined uniquely. In our definition, the structure of the advective term is retained. That is, the mediating mode is combined with the nabla operator by the inner product. Thus the mediating mode causes the energy transfer through the velocity field constituted by it. This characteristic of the unit is preferred in our definition.

For the Burgers equation, the definition of $\mathcal{T}(a : b \to c)$ is

$$\mathcal{T}(a : b \to c) \equiv -\frac{1}{3}\int u^{(a)}\left\{u^{(c)}\frac{\partial}{\partial x}u^{(b)} - u^{(b)}\frac{\partial}{\partial x}u^{(c)}\right\}dx. \tag{3.7}$$

We also define $\overline{\mathcal{T}}(b \to c)$ in the same way as the definition (3.6). Note that the constant before the integral differs from that in the definition (3.4), as they are chosen to be consistent with Eq. (3.3).

The unit can also be represented by means of wavelet coefficients, although it is defined by an integral of triple products of modes. For the simplest case where each mode is constructed by a single wavelet base, the unit is rewritten as follows:

$$\mathcal{T}(C : A \to B) = \hat{u}_{j_1}^{m_1}\hat{u}_{j_2}^{m_2}\hat{u}_{j_3}^{m_3}I(C : A, B), \tag{3.8}$$

$$I(C : A, B) \equiv -\frac{1}{3}\int \psi_{j_3}^{m_3}\left\{\psi_{j_2}^{m_2}\frac{\partial}{\partial x}\psi_{j_1}^{m_1} - \psi_{j_1}^{m_1}\frac{\partial}{\partial x}\psi_{j_2}^{m_2}\right\}dx, \tag{3.9}$$

where each of A, B and C denotes the mode defined by a single wavelet base, $\psi_{j_1}^{m_1}$, $\psi_{j_2}^{m_2}$, and $\psi_{j_3}^{m_3}$, and their coefficients are $\hat{u}_{j_1}^{m_1}$, $\hat{u}_{j_2}^{m_2}$, and $\hat{u}_{j_3}^{m_3}$, respectively.

In a similar way, units for higher spatial dimensions can also be rewritten by means of wavelet coefficients, although the result takes a more complicated representation because of the added parameters. Therefore our notation for the definition of the unit is more convenient than that with wavelet coefficients.

B. Comparison of our definition with that in Fourier-triad analysis

Here we try to explain the unit in the context of the triad interaction. In the Fourier basis, what we call "triad interaction" is naturally introduced, where the sum of modal energies conserves. On the other hand, as mentioned in Sec. II, the transfer function which satisfies the concept of the triad interaction is not defined trivially in non-Fourier bases. Then we have introduced the unit to construct a triad interaction which is naturally connected to that in the Fourier basis.

Now we consider a single triad where the sum of the energy changes of three modes is conserved due to nonlinear terms of governing equations such as convective terms of the Navier-Stokes equations or the Burgers equation. Note that we do not consider the energy exchange due to pressure here. In Fourier space, however, our triad

interaction without the pressure effect coincides with the traditional one because the energy exchange due to pressure vanishes as commented on in the Introduction:

$$\Delta E^{(a)} + \Delta E^{(b)} + \Delta E^{(c)} = 0, \tag{3.10}$$

where $\Delta E^{(a)}, \Delta E^{(b)}, \Delta E^{(c)}$ are the energy change of the three modes in consideration for infinitesimal time δt. Next, we introduce the energy transfers α, β, γ between any pair of them as shown in Fig. 3. Then $\Delta E^{(\ )}$ are described with α, β, γ as follows:

$$\begin{aligned} \Delta E^{(a)} &= (\gamma - \alpha)\delta t = 2T(a|b,c)\delta t, \\ \Delta E^{(b)} &= (\alpha - \beta)\delta t = 2T(b|c,a)\delta t, \\ \Delta E^{(c)} &= (\beta - \gamma)\delta t = 2T(c|a,b)\delta t. \end{aligned} \tag{3.11}$$

Since Eqs. (3.10) and (3.12) are not independent, one parameter f is needed to represent α, β, γ with $\Delta E^{(\ )}$ as

$$\begin{aligned} \alpha &= \tfrac{1}{3}\{\Delta E^{(b)} - \Delta E^{(a)}\}/\delta t + f, \\ \beta &= \tfrac{1}{3}\{\Delta E^{(c)} - \Delta E^{(b)}\}/\delta t + f, \\ \gamma &= \tfrac{1}{3}\{\Delta E^{(a)} - \Delta E^{(c)}\}/\delta t + f, \end{aligned} \tag{3.12}$$

where

$$f = (\alpha + \beta + \gamma)/3. \tag{3.13}$$

The parameter f is generally time dependent and denotes the net circulation flux in this triad. In our definition, f is 0 for 1D (e.g., the Burgers equation), but is not fixed for 2D or 3D. In the Fourier-triad analysis, the net circulation of energy, f, is kept also uncertain in each triad. In this sense, our definition is just an extension of the traditional one, but takes the simplest form. As a matter of fact, we can construct other units (see the Appendix for a unit with $f = 0$), but such units are too complicated to be interpreted physically. In any case, when we use a unit to analyze local interaction between modes, we should carefully estimate the energy transfer between them.

Finally we should remark on the selection rule of a triad. We can also construct the triad interaction with the units in the wavelet basis although any three wavelet modes can interact. In this paper, we basically deal with the local transfer function defined by (3.6), because they can be interpreted as the energy transfer between two modes as the usual treatment in the Fourier-triad analysis. It should be noted that generally a mode can be constituted by a set of wavelet bases, and the solution is divided into several orthogonal modes or subsets here.

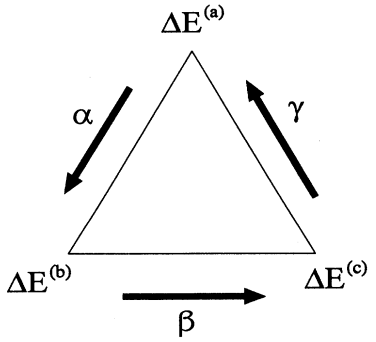

FIG. 3. Detailed balance of the three modes in the transfer term. The energy transfers between each two modes are α, β, γ, respectively.

C. Physical view of the local transfer function

In this subsection we will explain a physical view of the local transfer function defined in Sec. III A. As an example, we will deal with the enstrophy transfer of 2D turbulence because the vorticity field is scalar and this fact makes the problem more tractable. However, the result can be applied to more complicated cases easily.

The vorticity equation is

$$\frac{\partial \omega}{\partial t} = (\boldsymbol{u} \cdot \nabla)\omega + \nu \Delta \omega, \tag{3.14}$$

where ν is the kinetic viscosity and $\omega \equiv (\nabla \times \boldsymbol{u})|_z$ is the vertical component of vorticity. In 2D turbulence, the enstrophy $Q \equiv \int dS \omega^2/2$ is assumed to cascade.

We assume the vorticity field is decomposed into several orthogonal subspaces as

$$\omega = \omega^{(a)} + \omega^{(b)} + \cdots \tag{3.15}$$

and

$$\omega^{(a)} \equiv \sum_j \Omega_j^{(a)} f_j^{(a)}, \quad \omega^{(b)} \equiv \sum_j \Omega_j^{(b)} f_j^{(b)}, \ldots, \tag{3.16}$$

where $\{f_j^{(a)}\}, \{f_j^{(b)}\}, \ldots$ are sets of normalized bases constituting the modes $a, b, \ldots$, respectively and $\Omega_j^{(a)}, \Omega_j^{(b)}, \ldots$ are the coefficients of the bases. Note that $\int f_i^{(a)} f_j^{(b)} dS = \delta_{ab}\delta_{ij}$. For incompressible fluids, the local transfer function for enstrophy can be derived in the same way as the definitions (3.14) and (3.15):

$$\overline{T}_Q(a \to b) \equiv -\int dS \omega^{(b)} (\boldsymbol{u} \cdot \nabla)\omega^{(a)}. \tag{3.17}$$

It should be noted that if the velocity field $\boldsymbol{u}$, the mediating mode, is divergent-free and surface integrals on the boundaries vanish, the two terms of the integral in Eq. (3.4) become equivalent.

Assume the mode $\omega^{(a)}$ contains a part of a vortex structure. After an infinitesimal time δt, the structure is transformed by the velocity field as $\omega^{(a)'} \simeq \omega^{(a)} - \delta t(\boldsymbol{u} \cdot \nabla)\omega^{(a)}$ if the viscous effect is neglected. Here, $\omega^{(a)'}$ represents the total transform of the part of the structure contained in the subspace a initially and can be spanned by not only the subspace a but also other subspaces. Thus this transformation of the structure induces the variation of other modes. The jth vorticity variation of the amplitude of the mode b due to the transformation of the

structure $\omega^{(a)}$ in the infinitesimal time δt, $\Delta_j \Omega_a^{(b)} \to b$, is derived as

$$\Delta_j \Omega_{a\to b}^{(b)} \equiv \int f_j^{(b)} \{\omega^{(a)} - \delta t(\boldsymbol{u}\cdot\nabla)\omega^{(a)}\} dS$$
$$= -\delta t \int f_j^{(b)} (\boldsymbol{u}\cdot\nabla)\omega^{(a)} dS. \tag{3.18}$$

Then $\Delta Q_{a\to b}^{(b)}$, the variation of the enstrophy of the mode b due to the mode a in a unit time, is described as

$$\Delta Q_{a\to b}^{(b)} = \frac{1}{\delta t}\left\{ \sum_j \frac{1}{2}(\Omega_j^{(b)} + \Delta_j \Omega_{a\to b}^{(b)})^2 - \sum_j \frac{1}{2}(\Omega_j^{(b)})^2 \right\}$$
$$\simeq \frac{1}{\delta t} \sum_j \Omega_j^{(b)} \Delta_j \Omega^{(b)}$$
$$= -\sum_j \Omega_j^{(b)} \int f_j^{(b)} (\boldsymbol{u}\cdot\nabla)\omega^{(a)} \} dS$$
$$= -\int \omega^{(b)} (\boldsymbol{u}\cdot\nabla)\omega^{(a)} dS. \tag{3.19}$$

Therefore $\Delta Q_{a\to b}^{(b)}$ is equivalent to the local transfer function defined by (3.19). Moreover, the enstrophy decrease of the mode b absorbed into the mode a in a unit time, $\Delta Q_{b\to a}^{(a)}$, equals $-\Delta Q_{a\to b}^{(b)}$. Therefore we can consider that $\Delta Q_{b\to a}^{(a)}$ and the enstrophy transfer between the modes a and b are equivalent. This means that in this case our definition of the local transfer function is consistent with the physical view and also satisfies the detailed balance of the enstrophy transfer between two modes considered. We can apply this view also to the unit defined in (3.4) if the mediating mode, $\boldsymbol{u}^{(a)}$, is divergent-free.

For compressible fluids, the definition (3.17) is no longer valid. In this case, the enstrophy variation of the mode b due to the mode a, $\Delta Q_{a\to b}^{(b)}$, does not balance with that of the mode a due to the mode b, $\Delta Q_{b\to a}^{(a)}$, i.e., $\int dS \omega^{(b)}(\boldsymbol{u}\cdot\nabla\omega^{(a)}) \neq -\int dS \omega^{(a)}(\boldsymbol{u}\cdot\nabla\omega^{(b)})$. Moreover, it is meaningless to consider the local balance, because enstrophy is not a conserved quantity in the inviscid limit.

The simple physical view stated above is not applied to the Burgers equation, because it is a 1D model of compressible fluids. Nevertheless energy is conserved in the inviscid case, i.e., $\nu = 0$ [see Eq. (4.1)]. Thus the explanation for the unit given in Sec. III B still holds for the Burgers equation.

As mentioned in the Introduction, the pressure should be treated explicitly in wavelet analysis. However, the application of the triad interaction introduced in this paper to pressure is not straightforward, because the nonlinear effect due to pressure takes quite a complicated form with velocity. Thus we should introduce a new scheme or view to analyze the role of pressure on the transfer process. We will leave this issue to future works.

IV. APPLICATION OF WAVELET ANALYSIS TO THE BURGERS SHOCK

A. Simulation

In this section, we apply wavelet analysis to the Burgers equation:

$$\frac{\partial u}{\partial t} = -u\frac{\partial u}{\partial x} + \nu \frac{\partial^2 u}{\partial x^2}. \tag{4.1}$$

In the Burgers equation, turbulent states are described asymptotically by a set of shocks. A shock basically consists of in-phase fluctuations of all scales and its front is localized spatially. Thus, modal energies defined in the orthonormal wavelet basis concentrate around the front of the shock, i.e., only the coefficients of wavelet bases placed near the shock take values. According to the progression of the shock, excitations of modes propagate. Furthermore, the energies seem to be also transferred toward smaller scales around the shock. Here, we examine these energy transfer processes in view of both scale and position.

For this purpose, first we part the velocity field into five modes named "observer mode," "larger scale mode," "smaller scale mode," "left mode," and "right mode," respectively, as follows:

$$u(x) = u^{(\mathrm{obs})} + u^{(\mathrm{large})} + u^{(\mathrm{small})} + u^{(\mathrm{right})} + u^{(\mathrm{left})}. \tag{4.2}$$

If we make the "observer mode" constituted by a single wavelet base with $m = m_0 (0 < m_0 < N)$, $j = 0$, then the definitions of these modes are

$$u^{(\mathrm{obs})} \equiv \hat{u}_{j=0}^{m_0} \psi_{j=0}^{m_0}(x),$$
$$u^{(\mathrm{large})} \equiv u_0 + \sum_{m,j\in S_{\mathrm{large}}} \hat{u}_j^m \psi_j^m(x),$$
$$u^{(\mathrm{small})} \equiv \sum_{m,j\in S_{\mathrm{small}}} \hat{u}_j^m \psi_j^m(x), \tag{4.3}$$
$$u^{(\mathrm{right})} \equiv \sum_{m,j\in S_{\mathrm{right}}} \hat{u}_j^m \psi_j^m(x),$$
$$u^{(\mathrm{left})} \equiv \sum_{m,j\in S_{\mathrm{left}}} \hat{u}_j^m \psi_j^m(x),$$

where

$$S_{\mathrm{large}} = \{m, j | 0 \le m < m_0, 0 \le j \le 2^m\},$$
$$S_{\mathrm{small}} = \{m, j | m_0 < m \le N-1, 0 \le j \le 2^m\},$$
$$S_{\mathrm{right}} = \{m, j | m = m_0, 0 < j \le 2^{m-1} - 1\},$$
$$S_{\mathrm{left}} = \{m, j | m = m_0, 2^{m-1} \le j \le 2^m - 1\}. \tag{4.4}$$

The mean flow u_0 (a constant) is included in $u^{(\mathrm{large})}$ because it is interpreted as a far larger scale flow. Since the introduction of the mean flow corresponds to Galilean transformation of the system, the speed of the mean flow does not have special meaning at this stage. That is, its value does not affect results qualitatively. However, the

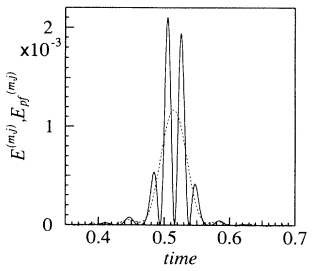

FIG. 4. The function $E^{(m=5,j=0)}(t)$ (solid line) and its phase-free counterpart $E_{pf}^{(m=5,j=0)}(t)$ (broken line).

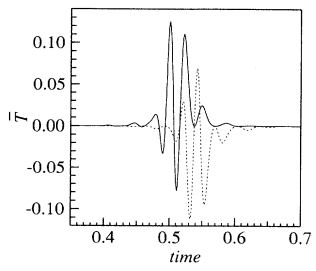

FIG. 6. Time series of $\bar{\mathcal{T}}$(left $\rightarrow$ obs) (solid line), $\bar{\mathcal{T}}$(right $\rightarrow$ obs) (broken line).

mean flow makes it clear that the time series of physical quantities observed by means of a wavelet is blurred by the spatial oscillation due to the phase as discussed in Sec. IV B 2. We examine the energy transfers between the "observer mode" and one of the other four modes with the transfer functions introduced in Sec. III numerically.

The Burgers equation is solved numerically by the fourth-order Runge-Kutta method for time and the pseudo-spectral method for space in the periodic region, $[0, 1]$. Aliasing terms are removed by the 2/3-rule method. We report the results obtained for 2^{10} modes, $dt = 1 \times 10^{-4}$, and $\nu = 1.5 \times 10^{-3}$. The initial condition adopted is $u(x) = 1 + 2\sin(2\pi x)$, and a single shock emerges and travels with the velocity of 1. Finally, for the "observer mode" we use $(m_0, j) = (5, 0)$ and also $(m_0, j) = (6, 0)$ for comparison. As mentioned in the last paragraph of Sec. II, the observer mode in a scale m is on the position $x = \Delta x_m/2$.

The time series of the energy due to the observer mode $(m_0, j) = (5, 0)$, $E^{(m=5,j=0)}(t)$, is shown in Fig. 4. Oscillation due to "phase" of a wavelet is observed. The transfer function, the time derivative of the modal energy function, also oscillates. Four time series of $\overline{\mathcal{T}}(\cdots \rightarrow$ obs), local transfer functions between "observer mode" and one of the other four modes, are displayed in Figs. 5 and 6. Although these four graphs show fast oscillations, $\overline{\mathcal{T}}$(large $\rightarrow$ obs) and $\overline{\mathcal{T}}$(left $\rightarrow$ obs) take positive values on average, while $\mathcal{T}$(small $\rightarrow$ obs) and $\mathcal{T}$(right $\rightarrow$ obs) take negative values.

Thus it is concluded that energy is transferred from larger to smaller scales and from left to right as the shock passes.

B. Numerical results on transfer functions

1. *The removal of information about phase*

As mentioned in the Introduction, the raw data of the transfer functions still contain the information about phase. In this subsubsection, we propose a way to separate substantial information from that about phase. Figure 7 show the absolute values of frequency components of the energies for the modes $(m = 5, j = 0)$ and $(m = 6, j = 0)$. Note that in this section ω denotes frequency, not vorticity.

Each of them takes two peaks. The higher peaks in Fig. 7 relate to the characteristic wave number of the wavelet basis, while the width of the lower peaks at $\omega = 0$ is concerned with the width of the wavelet basis in Fourier space. To see this, we consider how the energy of a shock with speed u_0 varies for observers within a scale m in wavelet space. From (2.12), Δx_m and Δk_m satisfy the relation

$$\Delta x_m \Delta k_m = C. \tag{4.5}$$

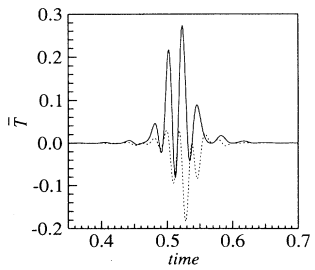

FIG. 5. Time series of $\bar{\mathcal{T}}$(large $\rightarrow$ obs) (solid line), $\bar{\mathcal{T}}$(small $\rightarrow$ obs) (broken line).

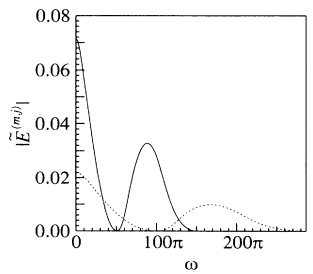

FIG. 7. The absolute values of Fourier coefficients of $E^{(m=5,j=0)}(t)$ (solid line) and $E^{(m=6,j=0)}(t)$ (broken line). The frequency of the higher peak in each graph is proportional to the scale parameter m.

When the shock passes the observer mode of (m, j), the energy of this mode oscillates with a characteristic frequency $\omega_m \sim 2u_0 k_m$, where k_m is the characteristic wave number ($\sim 2\pi 2^m$ in this case). Hence the propagation of the shock is observed as successive oscillations of the energy at adjacent grid points within a scale. This frequency characterized by ω_m corresponds to the higher peaks of the Fourier coefficients of the energy variations in Fig. 7.

On the other hand, the lower peaks have a width $\Delta\omega_m$ around $\omega = 0$. We will relate $\Delta\omega_m$ to Δx_m. The characteristic time in which the shock passes through the characteristic width Δx_m of a wavelet is estimated as $\Delta t_m \sim \Delta x_m / u_0$. Then $\Delta\omega_m$ is defined as follows:

$$\Delta\omega_m \sim \frac{1}{\Delta t_m} \sim \frac{u_0}{\Delta x_m} \sim \frac{u_0 \Delta k_m}{C}. \tag{4.6}$$

This means that the lower frequency part in the region $|\omega| \leq \Delta\omega_m/2$ represents relatively slow variation of the order of Δt_m, which is the substantial information about the pass of the shock. Therefore we should remove the high-frequency component of the time series of the energy of the mode to select the phase-free energy variation (PFE). It should be noted that even after removing phase, the total amount of energy transferred, the coefficient for $\omega = 0$, is unchanged.

Finally, we relate PFE to the phase-free transfer function. We define a way quantitatively to remove the phase of the energy $E^{(a)}(t)$ for the mode "a" as follows:

$$E_{pf}^{(a)}(t) = \int G(t - t') E^{(a)}(t') dt', \tag{4.7}$$

$$\begin{aligned} G(t) &\equiv \textstyle\int \tilde{G}(\omega) e^{-i\omega t} d\omega, \\ \tilde{G}(\omega) &\equiv \begin{cases} 1 & (|\omega| \leq \omega_0), \\ 0 & (|\omega| > \omega_0), \end{cases} \end{aligned} \tag{4.8}$$

where the subscript pf denotes the phase-free function. Note that ω_0 is the characteristic frequency at which the frequency components of $E^{(a)}(t)$ are divided into the substantial part and the fast oscillating one. We used $\omega_0 = 51\pi, 102\pi$ for the modes $(m = 5, j = 0), (m = 6, j = 0)$, respectively. The phase-free unit is also defined in the same way as the definition (4.8). From Eq. (3.3), the time derivative of PFE can be described with the phase-free unit as follows:

$$\frac{d}{dt} E_{pf}^{(a)}(t) = \sum_{b,c} \mathcal{T}_{pf}(b : c \to a)(t), \tag{4.9}$$

where

$$\mathcal{T}_{pf}(b : c \to a)(t) = \int G(t - t') \mathcal{T}(b : c \to a)(t') dt'. \tag{4.10}$$

The phase-free local transfer function can also be defined by the sum of the phase-free unit:

$$\overline{\mathcal{T}}_{pf}(c \to a)(t) = \sum_{b} \mathcal{T}_{pf}(b : c \to a)(t). \tag{4.11}$$

2. *The role of the mean flow in removing the phase*

In this subsubsection, we will comment on the methods of removing the "phase" intrinsic to the wavelet by comparing the temporal case with the spatial one. It should be noted that the problem on the intrinsic phase is a technical problem when using wavelets, and has no relation to physical considerations. There are two kinds of methods. One is the method proposed in this paper using temporal averaging. The essential part of this method is the introduction of a mean flow which corresponds to the Galilean transformation of the system. By this transformation, we can continuously observe the temporal variation of a single wavelet mode fixed in space. As reported in the next subsubsection, the time series of physical quantities observed is blurred by the continuous oscillation due to the phase. Though the characteristic frequencies (time scales) of the intrinsic oscillation and the substantial variation depend on the velocity of the mean flow, these characteristic frequencies are well separated for all nonzero values of the velocity. Thus by averaging the time series of physical quantities observed over the time scale of the fast intrinsic oscillation, we can remove the phase and obtain the substantial variation. We conclude that the mean flow does not play any essential role in the removal of the phase.

While we have dealt with the temporal case in this paper as preliminary work, it is not difficult to introduce a way of removing the spatial oscillations due to the phase by spatial averaging. Here we will explain the method briefly. Roughly speaking, this method is based on the spatial averaging over the length scale of the spatial oscillation due to the phase. We can extend a discrete wavelet to a continuous one based on the translational invariance of an orthonormal wavelet. Then the discrete position parameter j is extended to the continuous one, l. If l coincides with one of the discrete points j, the coefficient of the continuous wavelet coincides with that of the orthogonal wavelet. Thus we can relate the squared coefficient of the continuous wavelet, e.g., the energy, to that in the orthogonal wavelet space. Since the concrete way of spatial averaging is similar to that in the temporal case, we omit the details here.

Besides the technique for removing the phase for general applications of this analysis, there remain two issues to be settled, in which physical consideration is required in order to analyze turbulence in terms of wavelet-triad analysis. In the first stage it is required to define appropriate energy transfer functions as proposed here. We have confirmed the validity of our definitions by applying them to a single structure with well-defined phase velocity; the single Burgers shock can be immobilized by subtracting the mean flow. At this level, the results obtained by the temporal and spatial treatments are equivalent. We will report the latter results elsewhere. It should be noted that at this stage the phase velocity of a structure plays a physically important role because it induces the sweeping of the physical quantities around the structure.

In the next stage, we would have to define struc-

tures and their phase velocities in turbulence states, if they exit. Since structures are spatially distributed and their phase velocities may greatly differ, we cannot relate the temporal averaging to the spatial one by a simple Galilean transformation, even for a one-dimensional case. However, so far we have not completely established the required definitions of structures and their phase velocities.

3. *The details of substantial information*

In Fig. 8, time evolutions of $\overline{\mathcal{T}}_{pf}$(large $\rightarrow$ obs) and $\overline{\mathcal{T}}_{pf}$(small $\rightarrow$ obs) are shown. Both the positive value of $\overline{\mathcal{T}}_{pf}$(large $\rightarrow$ obs) and the negative value of $\overline{\mathcal{T}}_{pf}$(small $\rightarrow$ obs) mean that energy is transferred from a large scale to a small one.

The similar graphs of $\overline{\mathcal{T}}_{pf}$(left $\rightarrow$ obs) and $\overline{\mathcal{T}}_{pf}$(right $\rightarrow$ obs) as those in Fig. 8 are plotted in Fig. 9. The similar discussion can be applied to these transfer processes. That is, energy is transferred from left to right through the pass of the shock. The total amounts of energy transferred by both the processes are estimated by the values of the graphs at $\omega = 0$ in Fig. 10. The difference of energy between input and output is dissipated by the viscosity within the scale m. Compared with the transfer across scales, the transfer within the scale does not lose so much energy by dissipation seemingly. This is because the shock in this scale is kept quasisteady by the balance between input and output of energy.

Here we introduce a unit time $\Delta t_m = \Delta x_m/u_0$ in which a shock moves the distance between adjacent sites. For $m = 5$ and $u_0 = 1$, $\Delta t_m = 1/32$. The width of the peaks in Figs. 8 and 9 is the same order of Δt_m. By the way, these graphs do not take maxima at the time that the shock passes the observer mode. To see this in detail, let $t_{m,j}$ be the time that the shock passes $x = x_{m,j}$, the position of the observer mode. Because the shock emerged from the initial condition $2\sin(2\pi x)$ and is swept by the mean flow $u_0 = 1$, $t_{m,j} = (0.5 + x_{m,j})/u_0$ for $t > 0.5$. Then for the observer mode at $x_{m=5,j=0}$, $t_{5,0} \sim 0.516$ is earlier than the times for the maxima of these graphs. These discrepancies will be explained well in the following (see Fig. 11).

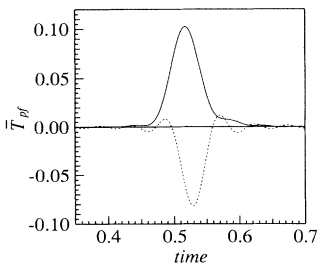

FIG. 8. Time series of $\bar{\mathcal{T}}_{pf}$(large $\rightarrow$ obs) (solid line) and $\bar{\mathcal{T}}_{pf}$(small $\rightarrow$ obs) (broken line).

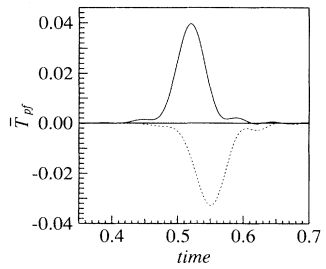

FIG. 9. Time series of $\bar{\mathcal{T}}_{pf}$(left $\rightarrow$ obs) (solid line) and $\bar{\mathcal{T}}_{pf}$(right $\rightarrow$ obs) (broken line).

Each of these transfer processes both within and across a scale consists of two elementary processes caused by the mean flow and the velocity intrinsic to the shock; the velocity jump exists across the shock. We have examined so far the local transfer functions whose mediating mode is the complete velocity field. The mediating mode originates from the convective term in the Burgers equation, and causes the energy transfer. Thus we can examine roles of the mediating mode in detail by dividing the velocity field $u(x)$ into the mean flow u_0 and the remainder $u'(x)$: $u(x) = u_0 + u'(x)$. We call them the mean mode and the remainder mode, respectively.

First, we discuss the energy transfer from the left mode to the observer mode within a scale, $\overline{\mathcal{T}}_{pf}$(left $\rightarrow$ obs), which is also divided into two units: $\mathcal{T}_{pf}$(mean : left $\rightarrow$ obs) and $\mathcal{T}_{pf}$(remainder : left $\rightarrow$ obs). In Fig.12, the time series of both units are shown. The shock passes the site of the observer mode at $t_{m,j=0} \sim 0.516$ for $m = 5$. The energy transfer caused by the mean flow, $\mathcal{T}_{pf}$(mean : left $\rightarrow$ obs), has the broad and positive peak of the width Δt_m around $t = 0.5$. During this period, the shock is between the site of the observer mode $x_{m,0}$ and its left next site $x_{m,-1}$ $(= x_{m,2^m-1})$. On the other hand, the energy transfer due to the remainder, $\mathcal{T}_{pf}$(remainder : left $\rightarrow$ obs), is roughly anti-symmetric around $t = 0.5$. The direction of the energy transfer due to the remainder changes its sign from negative to

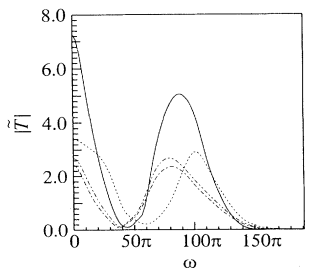

FIG. 10. The absolute values of Fourier coefficients of $\mathcal{T}(t)$'s for m. The energy transfers from the mode of large, small, left, and right are shown by solid line, broken line, dotted broken line, two-dotted broken line, respectively.

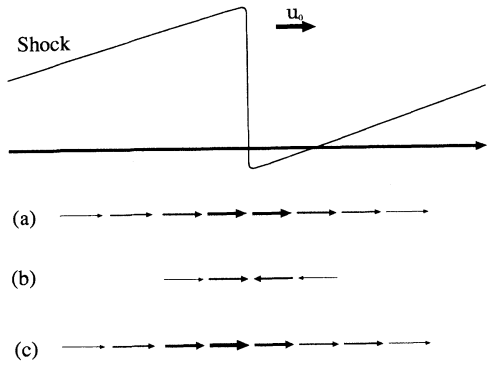

FIG. 11. Schematic view of the two elementary processes of the energy transfer within the same scale: (a) sweeping by the mean flow, (b) compression by the shock structure (velocity jump), (c) the sum of both processes; the total contribution.

positive at $t = 0.5$ when the shock is on the center between the observer's site and its left next site. From the symmetry of the situation, it is easily understandable that the transfers between the shock and the above two sites ($x_{m,0}$ and $x_{m,-1}$) coincide. Further, the transfer between the observer mode and the left mode turns into zero at $t = 0.5$ [$\sim \frac{1}{2}(t_{m=5,j=0} + t_{m=5,j=-1})$]. Therefore, we deduce that energy is concentrated to the center of the shock within the scale by the remainder: compression. As explained analytically in the next subsection, the transfer between the observer mode and the left adjacent site (strictly speaking, the mode assigned to this site) can approximate to $\mathcal{T}_{pf}$(remainder : left $\rightarrow$ obs).

The transfer from the right mode to the observer mode can also be decomposed into the transfers by the mean flow and the remainder: the sweeping and the compression (see Fig. 11). These transfers, units, are easily interpreted in comparison with those from the left to the observer mode. The transfer due to the mean flow has the broad and negative peak around $t = \frac{1}{2}(t_{m=5,j=0} + t_{m=5,j=1}) \sim 0.533$ when the shock is on the center between the observer $x_{m,0}$ and the right adjacent site $x_{m,1}$. The transfer due to the remainder changes its sign from positive to negative at $t = 0.533$. The time delay Δt_m

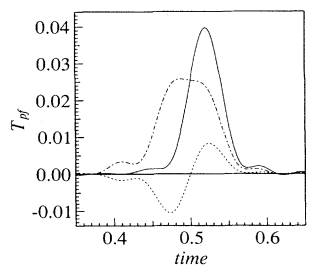

FIG. 12. Time series of $\mathcal{T}_{pf}$(mean : left $\rightarrow$ obs) and $\mathcal{T}_{pf}$(remainder : left $\rightarrow$ obs), $\overline{\mathcal{T}}_{pf}$(left $\rightarrow$ obs) (dash-dotted line, broken line, solid line, respectively).

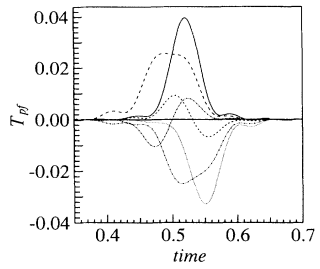

FIG. 13. Time series of $\mathcal{T}_{pf}$(mean : left $\rightarrow$ obs) and $\mathcal{T}_{pf}$(remainder : left $\rightarrow$ obs), $\overline{\mathcal{T}}_{pf}$(left $\rightarrow$ obs) (dashed line, broken line, solid line, respectively) and $\mathcal{T}_{pf}$(mean : right $\rightarrow$ obs), $\mathcal{T}_{pf}$(remainder : right $\rightarrow$ obs), $\overline{\mathcal{T}}_{pf}$(right $\rightarrow$ obs) (dash-double dotted line, dash-dotted line, dotted line, respectively).

between the zeros of $\mathcal{T}_{pf}$(remainder : left $\rightarrow$ obs) and $\mathcal{T}_{pf}$(remainder : right $\rightarrow$ obs) corresponds to the distance between these two centers, $x_{m,0} \pm \frac{1}{2}\Delta x_m$. The antisymmetry of $\mathcal{T}_{pf}$(remainder : right $\rightarrow$ obs) means also the energy compression (see Fig. 13).

The total transfer of the observer mode within this scale due to the mean flow is the sum of $\mathcal{T}_{pf}$(mean : left $\rightarrow$ obs) and $\mathcal{T}_{pf}$(mean : right $\rightarrow$ obs). This transfer takes a zero at $t = 0.5 + \Delta t_m$ when the shock is on the observer. At this time, the transfer changes its sign from positive to negative. That is, the pass of the energy blob accompanied with the shock is observed. The total transfers within a scale, $\overline{\mathcal{T}}_{pf}$(left $\rightarrow$ obs) and $\overline{\mathcal{T}}_{pf}$(right $\rightarrow$ obs), take relatively sharp peaks after the pass of the shock. This delay of the peak of each transfer is caused by the energy compression, and can be explained only by the decomposition of the transfer function used here.

Next, we examine the energy transfer from the large mode to the observer one: $\overline{\mathcal{T}}_{pf}$(large $\rightarrow$ obs) = $\mathcal{T}_{pf}$(mean : large $\rightarrow$ obs) + $\mathcal{T}_{pf}$(remainder : large $\rightarrow$ obs). These transfer functions are shown in Fig. 14. Contrary to the transfers within a scale, the transfer due to the mean flow, $\mathcal{T}_{pf}$(mean : large $\rightarrow$ obs), is antisymmetric. That is, before the pass of the shock, energy is transferred to the larger scale from the observer and then the same amount of energy is returned after the pass. We

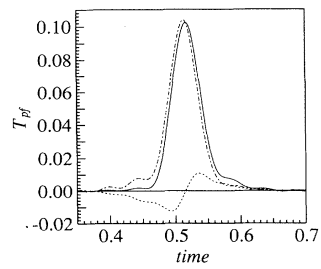

FIG. 14. Time series of $\mathcal{T}_{pf}$(mean : large $\rightarrow$ obs) (dash-dotted line), $\mathcal{T}_{pf}$(remainder : large $\rightarrow$ obs) (broken line) and $\overline{\mathcal{T}}_{pf}$(large $\rightarrow$ obs) (solid line).

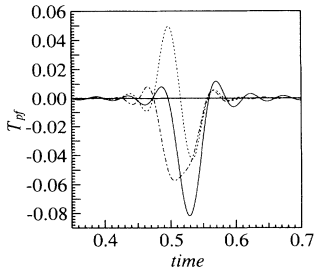

FIG. 15. Time series of $\mathcal{T}_{pf}$(mean : small $\rightarrow$ obs) (dash-dotted line), $\mathcal{T}_{pf}$(remainder : small $\rightarrow$ obs) (broken line), and $\overline{\mathcal{T}}_{pf}$(small $\rightarrow$ obs) (solid line).

cannot explain the physical meaning of this antisymmetric nature so far. Anyway, the mean flow affects even the transfer across scales. The transfer due to the remainder mode, $\mathcal{T}_{pf}$(remainder : large $\rightarrow$ obs), takes a sharp positive peak at $t = t_{m=5,j=0}$. This means that the energy is transferred from the large mode to the observer mode around the shock by the remainder. In this case, the former is relatively smaller than the latter, therefore the total transfer, $\overline{\mathcal{T}}_{pf}$(large $\rightarrow$ obs), is not shifted remarkably.

The transfer from the small mode to the observer mode is also decomposed into the transfers due to the mean flow and the remainder. In Fig. 15, time series of these transfers are plotted. The transfer due to the mean flow, $\mathcal{T}_{pf}$(mean : small $\rightarrow$ obs), is antisymmetric and changes its sign from positive to negative also at $t = 0.5 + \Delta t_m/2$. This means that some amount of energy of the small mode is given to the observer mode and then returned as the shock passes. The transfer due to the remainder, $\mathcal{T}_{pf}$(remainder : small $\rightarrow$ obs), takes a relatively broad and negative peak at $t = 0.5 + \Delta t_m/2$. That is, energy is transferred from the observer mode to the small mode. The total transfer, however, is affected by the mean flow effectively so that it is shifted further and gets narrower than $\overline{\mathcal{T}}_{pf}$(large $\rightarrow$ obs).

C. Analytical results for the sweeping effect

Because of the Galileian invariance of the Burgers equation, the mean flow moves a shock with a constant speed. That is, a blob of energy in a scale is simply swept within the scale. Thus some of $\mathcal{T}$(mean : $b \rightarrow c$) should express this sweeping; from the site of the blob to the just forward site energy is transferred by the mean flow. In this subsubsection we attempt to explain this analytically.

Let us consider scales where viscosity is negligible. Then the shock can be approximated by a step function:

$$\begin{aligned} u(x) &= [-\Theta(x - x_0) + \tfrac{1}{2}] + \hat{u}^{(0)} \\ &= -\int_{-\infty}^{x} \delta(x' - x_0)dx' + \tfrac{1}{2} + \hat{u}^{(0)}, \end{aligned} \tag{4.12}$$

where $\delta(x)$ is Dirac's delta function. The wavelet coefficient of the velocity field, $\hat{u}_j^m$, is represented as an integral of wavelet basis. To do this, we define a function $\hat{u}^{(m)}(y)$ as follows:

$$\begin{aligned} \hat{u}^{(m)}(y) &\equiv \int_{-\infty}^{\infty} u(x) 2^{\frac{m}{2}} \psi(2^m x - y)dx \\ &= 2^{1+\frac{m}{2}} \int_{-\infty}^{x_0} \psi(2^m x - y)dx \\ &= 2^{1+\frac{m}{2}} \int_{-\infty}^{x_0 - 2^{-m}y} \psi(2^m z)dz. \end{aligned} \tag{4.13}$$

Note that $\hat{u}^{(m)}(y)$ at $y = j$ (j is an integer) agrees with $\hat{u}_j^m$. The function $\hat{u}^{(m)}(y)$, which is shown in Fig. 16, oscillates around $y = x_0$ with its wavelength about 2. Thus $\hat{u}_j^m$ changes its sign in turn as $|j|$ increases and decays fast as j goes away from the shock. The main procedure is to calculate $\mathcal{T}$(mean : $b \rightarrow c$) when the passive and active mode are the wavelet modes of $(m_0, j_1), (m_0, j_2)$ $(j_1 \neq j_2)$, respectively. The mean flow is taken as the mediating mode,

$$\begin{aligned} \mathcal{T}(\text{mean} : j_1 \rightarrow j_2) &= -\hat{u}^{(0)} \hat{u}_{j_1}^{m_0} \hat{u}_{j_2}^{m_0} \frac{1}{3} \int \left\{ \psi_{j_2}^{m_0} \frac{\partial}{\partial x} \psi_{j_1}^{m_0} \right. \\ &\quad \left. - \psi_{j_1}^{m_0} \frac{\partial}{\partial x} \psi_{j_2}^{m_0} \right\} dx \\ &= \hat{u}^{(0)} \hat{u}_{j_1}^{m_0} \hat{u}_{j_2}^{m_0} \mathcal{T}_c^{(m_0)}(J), \end{aligned} \tag{4.14}$$

where $J \equiv j_2 - j_1$. Then $\mathcal{T}_c^{(m_0)}(J)$ is defined as follows:

$$\begin{aligned} \mathcal{T}_c^{(m_0)}(J) &\equiv -\frac{1}{3} \int \left\{ \psi_{j_2}^{m_0} \frac{\partial}{\partial x} \psi_{j_1}^{m_0} - \psi_{j_1}^{m_0} \frac{\partial}{\partial x} \psi_{j_2}^{m_0} \right\} dx \\ &= -\frac{2^{m_0}}{3} \left\{ \frac{1}{J}[2 - (-1)^J] - 2 \int_{\pi}^{\frac{4\pi}{3}} [4 \sin(2Jk) \right. \\ &\quad \left. - \sin(Jk)] \tilde{\phi}^2(k) dk \right\}, \end{aligned} \tag{4.15}$$

where $\tilde{\psi}_0$ and $\tilde{\phi}_0$ are introduced in Sec. II. As shown

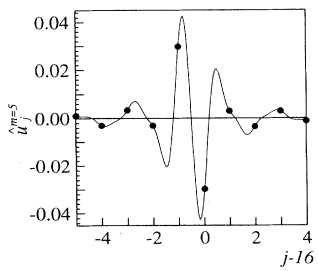

FIG. 16. The function $\hat{u}^{(m)}(y)$. Black circles are located at $2^{-m}j$ for integer j. The interval 2^{-m} is about half of the wavelength of this function.

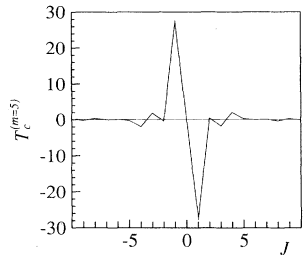

FIG. 17. The function $\mathcal{T}_c^{(m_0)}(j)$, which has large peaks at $j = \pm 1$.

in Fig. 17, $\mathcal{T}_c^{(m_0)}(J)$ has large peaks at $J = \pm 1$ and decreases rapidly as $|J|$ increases. Therefore the exchange of energy within a scale takes place mainly between adjacent modes such as $|j_1 - j_2| = 1$. In addition, $\hat{u}_j^m$ decreases faster than any power of the distance from the shock, and changes its sign site by site (see Fig. 16). This means that $\mathcal{T}(\text{mean} : j_1 \to j_2)$ has a large positive value around the shock when $j_2 - j_1 = 1$ and $u_0 > 0$. Thus we can conclude that the mean flow induces the energy transfer which corresponds to the sweeping of the shock. It should be noted that this conclusion can be extended to the situation where the large-scale velocity field works as mean flow locally.

V. SUMMARY AND CONCLUSION

The purpose of this study is to construct a method to observe transfer processes within and across scales by means of orthonormal wavelet analysis. We have also proposed a general expression of the energy transfer functions regardless of bases.

The most important ingredient of this method is the removal of the information about phase. Because we utilize orthonormal wavelet analysis, the energy of each wavelet mode is defined as half the squared wavelet coefficient as usual. The transfer observed in terms of this simple definition, however, shows more complicated variation than that expected by physical intuition. This is because the effect of the phase intrinsic to a wavelet base function is not explicitly treated.

To reveal the phase oscillation, we have analyzed time series of the transfer functions due to a shock traveling with a constant speed as an example. The speed of a shock can be controlled by Galilean transformation of a system. Since the phase is represented by higher frequency components of the time series, we can separate the substantial information from the phase by cutting off the higher frequency components.

After removing phase, we have examined the energy transfers within and across a scale. Each local transfer function is decomposed into two units due to the mean flow and the remainder, i.e., the velocity intrinsic to the shock. For the transfers within a scale, the mean flow sweeps the energy from left to right according to the progression of the shock. The velocity intrinsic to the shock induces the compression of energy to the shock. The mean flow causes even the transfers across a scale, which are not substantial. Thus we should carefully evaluate substantial transfers through scales. Although, in the case of the shock traveling steadily, the separation of the mean flow from the intrinsic velocity is trivial, in a real situation the separation should be performed carefully. We are trying to define the local mean flow systematically by means of wavelet transformation.

The extension of the present method, the removal of phase by spatial averaging over the length scale of the spatial oscillation, to field data is underway and seems to be successfully settled. In this extension, field data are spatially filtered in terms of a continuous wavelet, which was discussed in Sec. IV B 2. This method may inform us about spatial distribution of the "local transfer" even for a single snapshot of fields. We are also applying these methods to 2D Navier-Stokes turbulence and free convective turbulence [11]. We have found transfer processes similar to ones discussed in this paper. These results will be reported in a forthcoming paper.

ACKNOWLEDGMENTS

The authors would like to express their cordial thanks to Professor Procaccia for valuable discussions and comments. This work was supported in part by a Grant-in-Aid (No. 06740341) from the Ministry of Education, Science and Culture of Japan.

APPENDIX: ANOTHER DEFINITION OF THE UNIT

It is pointed out in Sec. III B that the unit cannot be defined uniquely; the one-third of the cyclic sum of three units in a triad, f, remains uncertain in the triad interaction. For example, we can define a unit with $f = 0$ as follows:

$$\mathcal{T}_{\text{new}}(a : b \to c) \equiv \mathcal{T}(a : b \to c) - F, \tag{A1}$$

where $F \equiv \frac{1}{3}\{\mathcal{T}(a : b \to c) + \mathcal{T}(b : c \to a) + \mathcal{T}(c : a \to b)\}$.

The sweeping works as a part of the energy transfer, but it is not substantial. Thus we have defined the unit in Sec. III by which the sweeping effect can be separated. However, the additional term introduced in this appendix makes this characteristic of the unit obscure. Think of the case that the mediating mode can be regarded as a constant flow (i.e., large-scale flow) and the other two modes are in a same and smaller scale but at different positions. The original unit can represent the sweeping effect trivially, but the new unit does not give such a simple interpretation because of its complexity.

[1] Y. Meyer, in *Wavelets*, edited by J. M. Combes, A. Grossmann, and Ph. Tchamitchian (Springer, Berlin, 1988), p. 21.
[2] M. Yamada and K. Ohkitani, Prog. Theor. Phys. **83**, 819 (1990); Fluid Dyn. Res. **8**, 101 (1991).
[3] C. Meneveau, Phys. Rev. Lett. **66**, 1450 (1991); J. Fluid Mech. **232**, 469 (1991).
[4] M. Farge, Annu. Rev. Fluid Mech. **24**, 395 (1992).
[5] F. Waleffe, Phys. Fluids A **4**, 350 (1992); **5**, 677 (1993).
[6] Y. Zhou, Phys. Fluids A **5**, 2511 (1993).
[7] J. A. Domaradzki and J. Rogallo, Phys. Fluids A **2**, 413 (1990).
[8] J. G. Brasseur and Q. Wang, Phys. Fluids A **4**, 2538 (1992).
[9] K. Ohkitani, Phys. Fluids A **3**, 1598 (1990).
[10] G. L. Eyink, Physica D **78**, 222 (1994).
[11] S. Toh and E. Suzuki, Phys. Rev. Lett. **73**, 1501 (1994).
[12] S. Toh, J. Phys. Soc. Jpn. **64**, 685 (1995).
[13] R. H. Kraichnan, Phys. Fluids **10**, 1417 (1967).
[14] M. E. Maltrud and G. K. Vallis, Phys. Fluids A **3**, 1760 (1991).
[15] D. E. Newland, Proc. R. Soc. London **443**, 203 (1993).
[16] R. L. Schult and H. W. Wyld, Phys. Rev. A **46**, 7953 (1992).
[17] K. Ohkitani and S. Kida, Phys. Fluids A **4**, 794 (1992).
[18] J. G. Brasseur and C. Wei, Phys. Fluids A **6**, 842 (1994).